Hindawi
Journal of Electrical and Computer Engineering
Volume 2018, Article ID 3498491, 9 pages
https://doi.org/10.1155/2018/3498491

Research Article

Analysis of Transient Voltage Stability in a Low Voltage Distribution Network Using SST for the Integration of Distributed Generations

Sheng Li, Zhihao Zhou, Qiqi Shan, and Jiani An

School of Electric Power Engineering, Nanjing Institute of Technology, Nanjing 211167, China

Correspondence should be addressed to Sheng Li; lisheng_njit@126.com

Received 17 February 2018; Revised 19 April 2018; Accepted 22 April 2018; Published 3 June 2018

Academic Editor: Chi-Seng Lam

Models of a low voltage distribution network using a typical tertiary-structure solid state transformer (SST) for the integration of distributed generations (DGs) and a conventional low voltage distribution network integrated with DGs were established to study the transient voltage stability issue, using the power system simulation software PSCAD. Effects on the transient voltage stability of the load bus and DC bus in the SST system are analyzed when grid-side cable line faults (such as short circuit and line disconnection) occur or the total output of DGs drops greatly. The results show that, comparing with the conventional system, the SST has apparent advantages on enhancing the transient voltage stability of load bus while facing different disturbances, even though SST has to regulate the voltage passively. Short circuit faults at different location of the grid-side line have different effects on the transient voltage stability, while the effect of disconnection fault is not related to fault location. Moreover, the DC bus voltage is easy to keep climbing continually when short circuit fault of the line occurs that is close to the SST input stage or disconnection fault occurs at any location of the line. If a battery energy storage station is installed, the transient voltage stability of DC bus and load bus will be improved effectively because of the regulation function of battery storage.

1. Introduction

With the technologies related to new energy generation being maturing day by day and the construction of the energy internet being pushed forward constantly [1–3], penetrations of distributed generations (DGs) in the distribution network are increasing gradually [4, 5]. Before the electric power grid and other energy networks connecting with each other and forming an energy internet, building a green smart grid with the core of energy routers to accept large-scale renewable energy sources widely is one way to construct the energy internet [6]. The intelligent dispatching and controlling center of the energy internet is the energy router [7], whose core is a high-frequency coupled device called solid state transformer (SST) based on the advanced power electronic technology [8].

The output of DG is random and the configuration of the distribution network integrated with DGs is complex, which can influence the stability of the distribution network [9, 10]. Reference [11] pointed out that the voltage stability issue does exist in distribution networks integrated with photovoltaic cell power, and the voltage instability phenomenon can be solved effectively by photovoltaic inverter reactive power support [2, 11]. A typical simulation model that a distributed photovoltaic power station is directly integrated into a low voltage distribution network was established in [12], and the effects were analyzed on the transient voltage stability of load bus when the faults such as short circuit and line disconnection occur or the output of distributed photovoltaic power plant drops greatly. In [13], the impacts of large-scale photovoltaic generation on the steady state voltage stability of distribution system were studied, and the conclusion that the photovoltaic modules have to operate in the reactive power support mode to improve the system voltage stability was obtained. In [14], a DC microgrid containing photovoltaic cell, wind turbine, and fuel cell was proposed and connected to the low voltage distribution network under variable load demands, and the simulation results showed that the voltage

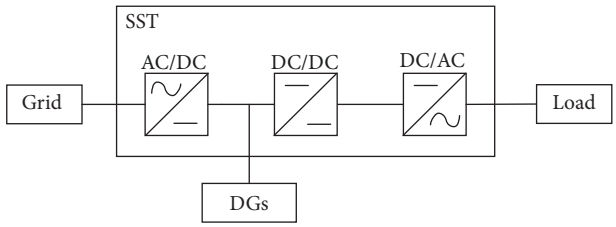

Figure 1: A typical tertiary-structure solid state transformer.

stability of DC bus can be maintained at different operating modes. In [15], a method that can enhance the transient voltage stability of a real distribution network with wind power was proposed, by means of optimal rating and location of the static synchronous compensator (STATCOM).

When using a SST for the integration of DGs and the distribution network, on the part of the grid, the ability of adopting the DGs will be enhanced and the situation of voltage oscillation and instability will be avoided. In this paper, a simulation model of a 0.38 kV low voltage distribution network which uses a typical SST for the integration of DGs was established using the power system simulation software PSCAD/EMTDC, and effects on the transient voltage stability of the system while facing various disturbances are studied. The advantages of the transient voltage stability using a SST for the integration of DGs are analyzed, and the differences between whether there is a battery energy storage station are discussed.

2. Modeling and Control Strategy of SST

As shown in Figure 1, a typical tertiary-structure SST is chosen for discussion, which consisted by a AC/DC unit, a DC/DC unit, and a DC/AC unit. The three units are input stage, isolation stage, and output stage, respectively. To realize the bidirectional power flow, the full-controlled device, IGBT, is used for building the SST [16].

In this paper, a voltage-source PMW rectifier is chosen as the input stage of SST, which can rectify the 0.38 kV AC of the low voltage distribution network to 0.78 kV DC.

The dual-loop decoupled control strategy is chosen for the input stage [17]. The voltage orientation control strategy based on d-q rotating coordinate system is selected for the voltage loop, and the direct current control is adopted for the current loop. The grid-side power factor can be corrected according to the control goal. The control equations of the SST input stage are

$$\begin{aligned} i_{1d}^{*} &= \left(K_{\mathrm{P1}} + \frac{K_{\mathrm{I1}}}{s}\right)\left(U_{\mathrm{dc}}' - U_{\mathrm{dc}}\right) \\ i_{1q}^{*} &= 0 \\ u_{1d}^{*} &= u_{1d} + \omega L i_{1q} - \left(K_{\mathrm{P2}} + \frac{K_{\mathrm{I2}}}{s}\right)\left(i_{1d}^{*} - i_{1d}\right) \\ u_{1q}^{*} &= u_{1q} - \omega L i_{1d} - \left(K_{\mathrm{P2}} + \frac{K_{\mathrm{I2}}}{s}\right)\left(i_{1q}^{*} - i_{1q}\right), \end{aligned} \tag{1}$$

where i_{1d}^{*} and i_{1q}^{*} are the grid-side current command values in d-q coordinate system and i_{1d} and i_{1q} are the actual values; u_{1d}^{*} and u_{1q}^{*} are the grid-side voltage command values in d-q coordinate system and u_{1d} and u_{1q} are the actual values; U_{dc}', U_{dc} are the reference voltage and actual voltage of DC bus, respectively; K_{P1}, K_{I1}, K_{P2}, and K_{I2} are the parameters of PI controllers; L is the filter inductance of SST input stage.

In isolation stage, the 0.78 kV DC is converted to a high-frequency AC square wave and coupled to the secondary side of a high-frequency isolated transformer which is used to isolate the original side and subside. Then, the high-frequency AC will be rectified to 0.78 kV DC.

In the output stage, the 0.78 kV DC is inverted to 0.38 kV AC for power supplies. The dual-loop decupled control strategy with the voltage and current feedforward is adopted for the control [18]. The control equations of the SST output stage are

$$\begin{aligned} i_{2d}^{*} &= i_{2d} - \omega C_f u_{2q} + \left(K_{\mathrm{P3}} + \frac{K_{\mathrm{I3}}}{s}\right)\left(u_{2d}' - u_{2d}\right) \\ i_{2q}^{*} &= i_{2q} + \omega C_f u_{2d} + \left(K_{\mathrm{P3}} + \frac{K_{\mathrm{I3}}}{s}\right)\left(u_{2q}' - u_{2q}\right) \\ u_{2d}^{*} &= u_{2d} - \omega L_f i_{2q} + \left(K_{\mathrm{P4}} + \frac{K_{\mathrm{I4}}}{s}\right)\left(i_{2d}^{*} - i_{2d}\right) \\ u_{2q}^{*} &= u_{2q} + \omega L_f i_{2d} + \left(K_{\mathrm{P4}} + \frac{K_{\mathrm{I4}}}{s}\right)\left(i_{2q}^{*} - i_{2q}\right), \end{aligned} \tag{2}$$

where i_{2d}^{*} and i_{2q}^{*} are the load current command values in d-q coordinate system and i_{2d} and i_{2q} are the actual values; u_{2d}^{*} and u_{2q}^{*} are the load bus voltage command values in d-q coordinate system, u_{2d}' and u_{2q}' are the reference values, and u_{2d} and u_{2q} are the actual values; K_{P3}, K_{I3}, K_{P4}, and K_{I4} are the parameters of PI controllers; L_f, C_f are the filter inductance and capacitance of SST output stage, respectively.

3. Model of Low Voltage Distribution Network Integrated with DGs

A conventional system model of a low voltage distribution network integrated with DGs (including distributed photovoltaic and wind power) is established using the power system simulation software PSCAD, as shown in Figure 2. $\dot{U}_1$ and $\dot{U}_2$ are the voltage of Bus 1 and Bus 2, respectively. The impedance of the cable is $R + jX$ and the value is $0.096 + j0.015\ \Omega$. The power from the low voltage distribution network is noted as $P_1 + jQ_1$, the power flow from the network to Bus 2 is noted as $P_2 + jQ_2$. The outputs of photovoltaic power plant and wind power farm are $P_{\mathrm{pv}} + jQ_{\mathrm{pv}}$ and $P_{\mathrm{wind}} + jQ_{\mathrm{wind}}$, respectively; the absorbed power of the three-phase induction motor and the static load are $P_M + jQ_M$ and $P_s + jQ_s$, respectively.

Some ancillary facilities such as reactive power compensation devices and inverters of photovoltaic or wind power systems can be left out because of the structure and flexible control characteristics of SST, and the DGs can be directly connected to the DC bus. The model of a low voltage distribution network using a SST for the integration of DGs is shown in Figure 3.

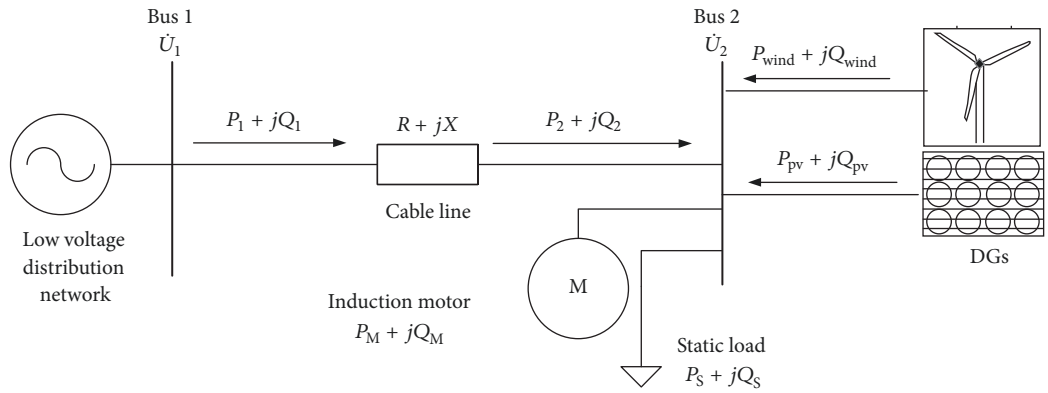

Figure 2: Model of conventional low voltage distribution network integrated with DGs.

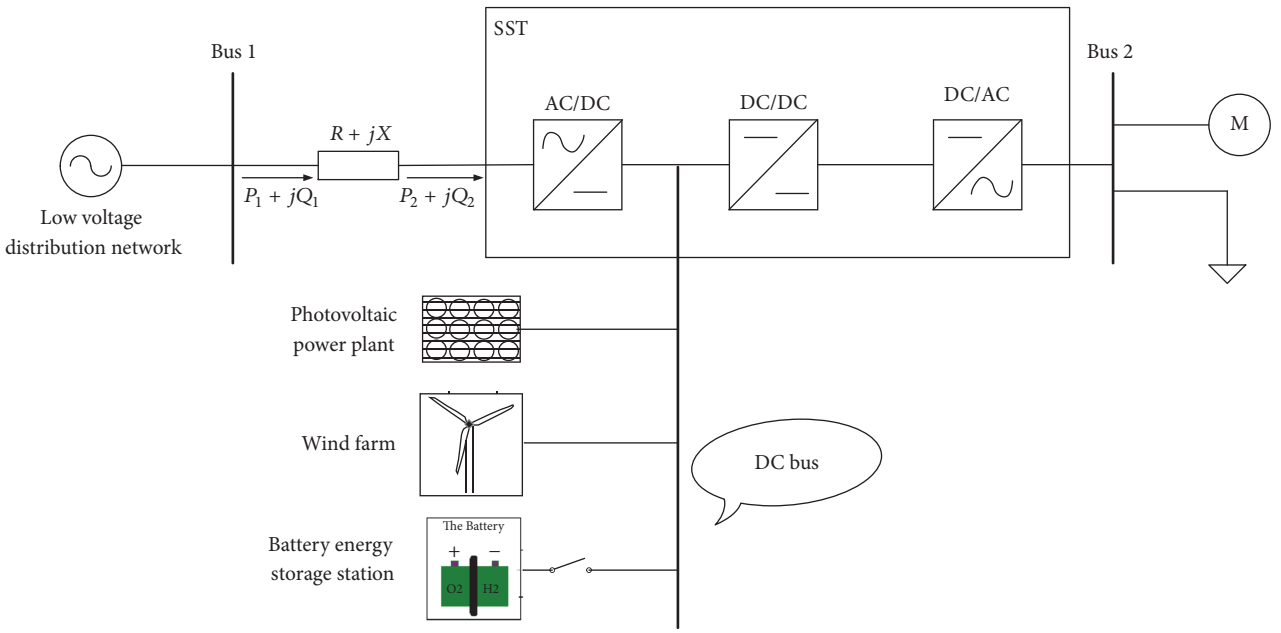

Figure 3: Model of low voltage distribution network integrated with DGs using SST.

In Figures 2 and 3, the rated capacities of the photovoltaic power station and the wind power plant both are 260 kW. The loads are composed of two parts of static load (including a constant resistance load and a constant impedance load) and a three-phase induction motor. The rated power of the constant resistance R_{s1} is 90 kW; the rated power of the constant impedance $R_{s2} + jX_{s2}$ is 60 kVA; the rated capacity of the three-phase induction motor is 49.5 kVA.

During the simulation analyses, the environmental temperature is 298.15 K, the light intensity is 1000 W/m^2, the wind speed is 11 m/s, and these values will vary in a certain rage. When the system operates normally, the absorbed active and reactive power of the induction motor are about 46 kW and 23 kvar, respectively; the absorbed active and reactive power of the constant impedance load are about 48 kW and 35 kvar, respectively. The grid-side unity power factor is realized due to the control strategy of the SST input stage.

4. Effects on Transient Voltage Stability of Grid-Side Line Faults

The research results show that short circuit fault of grid-side cable line at different location has different effect on the system transient voltage stability because of the control function of the SST input stage, while line disconnection fault is not associated with the fault location.

The schematic diagram of fault position is shown in Figure 4. The grid-side cable line is divided into Line 1 and Line 2 equivalently, by the signal collection device which monitors the distribution network. Line 1 contains only a small part of lines connecting the signal collection device and the SST input stage in practice, and its fault possibility is much lower. Line 2 contains the whole external distribution network lines which are so complex that their fault possibility is very high.

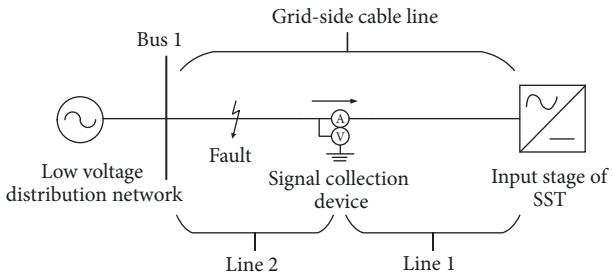

Figure 4: Schematic diagram of line fault location.

To save space and take the aesthetics into consideration, most urban low voltage distribution networks use cable lines. Insulation aging or damage is the main cause of cable faults.

4.1. Short Circuit Fault Occurs at Line 1. Line 1 may have short circuit faults though there are fewer lines in it. Once the fault occurs, each stage of the SST has to regulate the voltage passively. Therefore, we focus on the influence on the system transient voltage stability when different short circuit faults occur at Line 1.

Take the typical single-phase grounding short circuit fault as an example. Now set the simulation time as 2 s. After time $t = 0.4$ s, the system enters stable operation. When $t = 0.6$ s, single-phase grounding short circuit fault occurs at the midpoint of Line 1, and the fault duration is 0.1 s. The relay protection acts and removes the fault line when $t = 0.65$ s. We focus on the system transient voltage stability when the cut line is no longer reinput because 0.38 kV low voltage cable line has generally no reclosing device.

After the line is cut off, the grid loses power and the DGs enter the state of isolation island operation. We do this research on the condition that the outputs of DGs are rich and can meet the need of local loads. When the single-phase grounding short circuit fault occurs, the response curves of load bus voltage and absorbed powers of induction motor in the conventional DGs grid-connected system (shown in Figure 2), the response curves of load bus (Bus 2) voltage, absorbed powers of induction motor, and DC bus voltage are shown in Figure 5.

In general, if a 0.38 kV AC bus voltage in low voltage distribution network is lower than 0.9 pu or higher than 1.1 pu after a large disturbance for more than the specified limit time (e.g., 1 s or above), it can be considered that the low voltage AC bus is transient voltage instability [12]. In this paper, the transient voltage stability of low voltage DC bus obeys the same rules, too.

As can be seen from Figures 5(a) and 5(b), for the conventional system, after the single-phase grounding short circuit fault occurs and the relay protection acts, the load bus voltage drops rapidly to 0.8 pu or less, and the load bus is considered to be unstable, thus causing the active and reactive power absorbed by induction motor to have oscillations and finally to be below rated values (rated active power is 1 pu and rated reactive power is 0.5 pu). The limitation of the conventional system is that the inverter control function of DGs is simple, and the transient voltage stability of load bus cannot be guaranteed while facing disturbances.

In this paper, the DGs' inverters adopt outlet voltage control strategy; simulation results show that the transient voltage stability of load bus cannot be maintained by the inverters without the support of power grid.

If the inverters adopt constant power control strategy, the outputs of DGs will remain constant under the normal environment after the disturbances. After the relay protection acts, the load bus has the equation according to the power balance:

$$P_{\text{pv}} + P_{\text{wind}} = P_M + P_S = P_M + \left(\frac{1}{R_{s1}} + \frac{R_{s2}}{R_{s2}^2 + X_{s2}^2} \right) U_2^2 \quad (3)$$

It can be seen from Formula (3), in the case of rich outputs of DGs, the load demand can be met, so the load bus voltage recovers quickly. Accordingly, the absorbed active power of induction motor begins to fall down after the oscillation. From Formula (3), we can find that U_2 will be lifted once P_M starts to decrease, eventually causing the load bus voltage to climb continually. And at this time, the load bus is still considered to be transient voltage instability. It is necessary to abandon the photovoltaic and wind power to protect the motor in time.

The effectiveness of the control strategy of SST on the transient voltage stability can be seen from Figures 5(a) and 5(b), which reflects the SST's better ability of maintaining transient voltage stability while facing disturbances. Though the fault is close to the SST input stage, active control cannot be taken by the SST to stabilize the grid-side surge current and the current has to be regulated passively and the load bus voltage can recover to the original rated value and maintain the stability after experiencing rapid sag. Therefore, the absorbed powers of induction motor can recover to the original rated values too.

As shown in Figure 5(c), although the SST can maintain the voltage stability of load bus by passive regulation, if there is no a battery energy storage station installed in the DC bus, the DC bus voltage will keep climbing because the outputs of DGs cannot be transmitted to the grid. At this time, we can consider that the DC bus loses its transient voltage stability. It is harmful to the security and stability of the system and the photovoltaic and wind power will have to be abandoned.

The battery energy storage station plays an important role in stabilizing the load bus voltage and DC bus voltage. As shown in Figure 5, in the DGs grid-connected system based on SST, the battery energy storage station can stabilize the load bus voltage and DC bus voltage greatly after the shot circuit fault occurs, and there is merely a slight oscillation. After the relay protection acts, the DC bus voltage is regulated to the original rated value because of the function of energy storage station, avoiding the voltage climbing phenomenon.

Simulation results show there are similar conclusions when other short circuit faults occur at Line 1; for instance, the response curves of three-phase short circuit occurring at midpoint of Line 1 are shown in Figure 6.

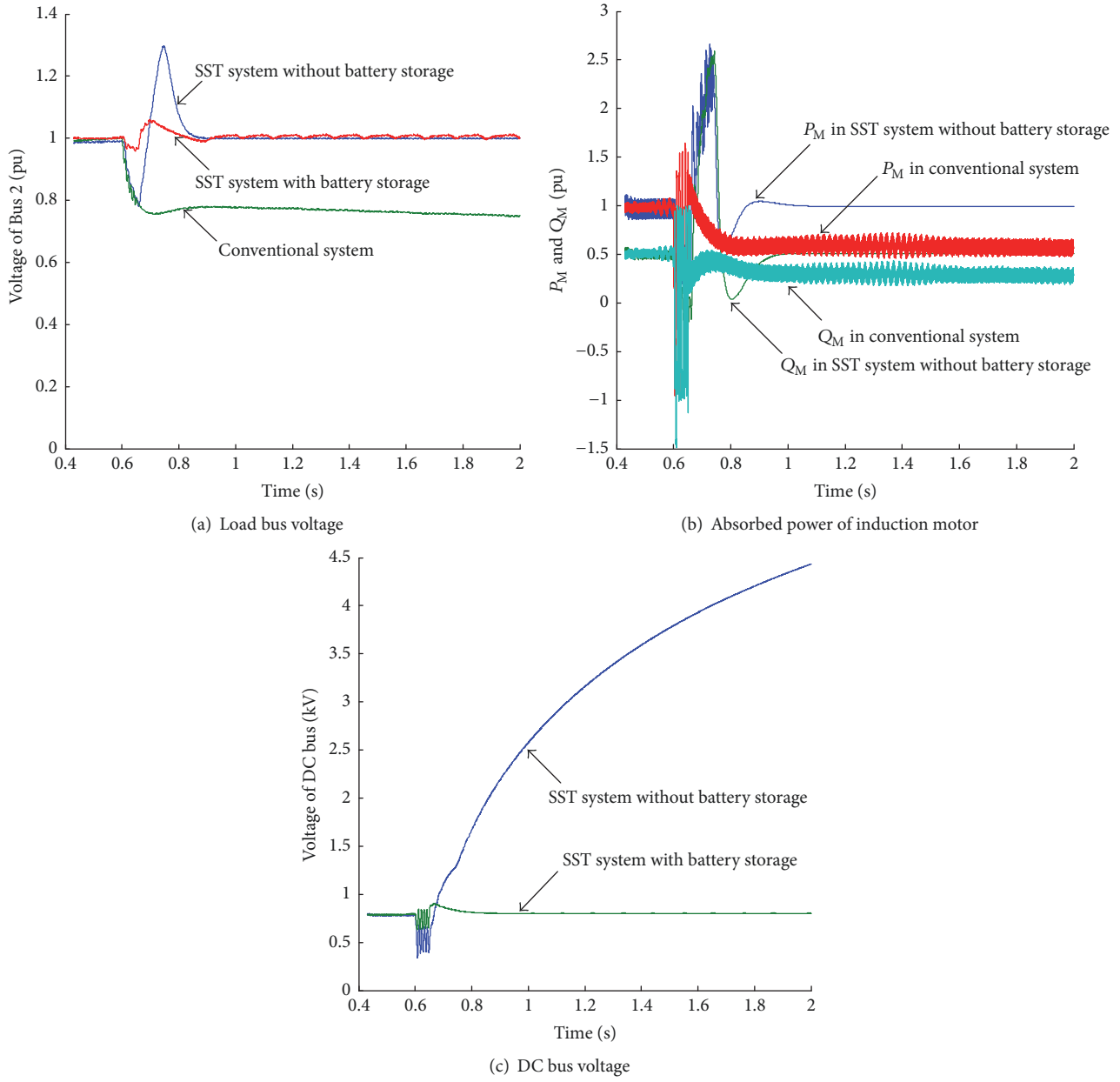

(a) Load bus voltage

(b) Absorbed power of induction motor

(c) DC bus voltage

FIGURE 5: Response curves when single-phase grounding short circuit fault occurs at the midpoint of Line 1.

4.2. Short Circuit Fault Occurs at Line 2. If short circuit fault occurs at Line 2, the information can be picked up and the surge current can be steadied by the active control of the SST input stage, and it merely has little effect on the load bus voltage and DC bus voltage even if the most serious three-phase short circuit fault occurs, as shown in Figure 7.

4.3. Disconnection Fault Occurs at Any Location of Gird-Side Line. When the line disconnection fault occurs at any location of the gird-side line (including Line 1 and Line 2), we can draw similar conclusions with the condition that short circuit faults occurs at Line 1. Taking the disconnection occurring at the midpoint of Line 1, for example, the response curves are shown in Figure 8.

5. Impact of Great Drop of DGs' Total Output on Transient Voltage Stability

The output of DG is affected by the weather greatly. The sudden changes in light intensity and wind speed will cause sudden changes in the outputs of photovoltaic power plant and wind farm, respectively, which will affect the transient voltage stability of the system.

Considering the most adverse weather condition, when the light intensity drops greatly and the wind turbine drops out because wind speed is too large, the sudden great drop of DGs' total output can cause the load bus voltage to be instability. For the conventional system shown in Figure 2, supposing that the total load power is $P_L + jQ_L$ and the total

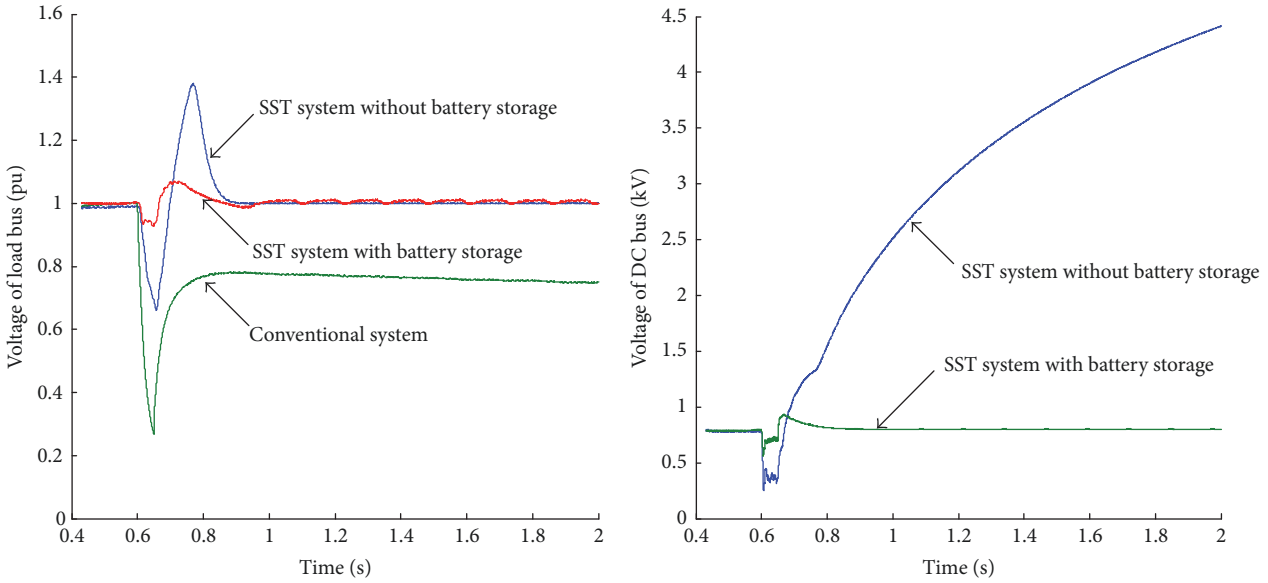

(a) Load bus voltage (b) DC bus voltage

Figure 6: Response curves when three-phase short circuit fault occurs at the midpoint of Line 1.

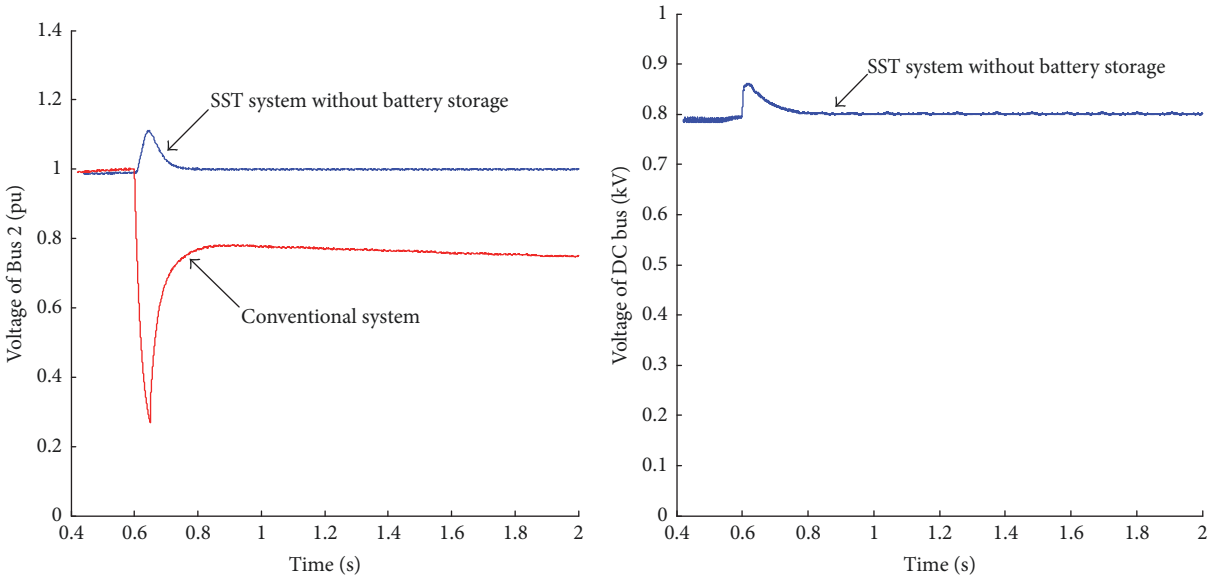

(a) Load bus voltage (b) DC bus voltage

Figure 7: Response curves when three-phase short circuit fault occurs at the midpoint of Line 2.

output of DGs is $P_\Sigma + jQ_\Sigma$, the load bus voltage drops to U_2' when the DGs' total output drops to 0 suddenly; there will be [12]

$$U_2 - U_2' = \frac{P_\Sigma R + Q_\Sigma X}{U_2} + \left(P_L R + Q_L X\right)\left(\frac{1}{U_2'} - \frac{1}{U_2}\right) \quad (4)$$

Since both photovoltaic and wind power have maximum power control, Q_Σ is almost 0. Suppose the voltage drop ratio is a; that is, $U_2' = aU_2$. Put $Q_\Sigma = 0$ and $U_2' = aU_2$ into Formula (4), we can get the following:

$$P_\Sigma = \frac{(1-a)U_2^2 - (1/a - 1)\left(P_L R + Q_L X\right)}{R} \quad (5)$$

In Formula (5), if U_2 is the rated value (1 pu), then a takes 0.9. And we can get the upper limit approximate value of total output active power of DGs that is just right for maintaining the system transient voltage stability when the total output

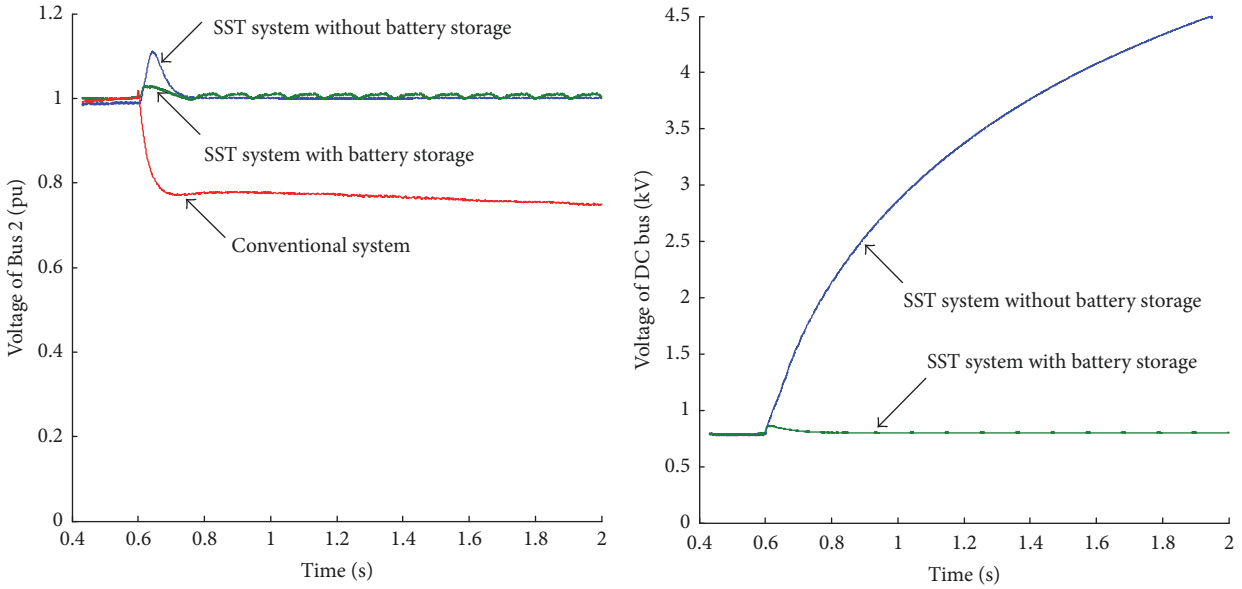

(a) Load bus voltage

(b) DC bus voltage

Figure 8: Response curves when disconnection fault occurs at the midpoint of Line 1.

drops to 0. When the DGs' total output is equal or greater than the upper limited approximate value in the actual operation of the system and drops to 0 suddenly, the load bus will lose its transient voltage stability in general.

Using the parameters in the conventional system to calculate according to Formula (5), it will figure out that the upper limit approximate value of DGs' total output is 150 kW as a takes 0.9 (because U_2 is very close to 1 pu). Now, the total output of DGs in the conventional system and the SST system is set to be 150 kW, respectively. The simulation time is set to be 2 s, and the photovoltaic and wind power suddenly drop to 0 at $t = 0.6$ s. The response curves are shown in Figure 9.

It can be known from Figures 9(a) and 9(b) that the load bus voltage in the conventional system is unstable after the great drop of DGs' total output occurs, and the voltage drops to about 0.88 pu which is almost matching with the theoretical value (0.9 pu), while in the SST system, the load bus and DC bus recover transient voltage stability quickly. When it comes to the SST system with a battery energy storage station, the voltages of load bus and DC bus are almost not affected by the disturbance. As can be seen from Figure 9(c), for the SST system without a battery energy storage station, before the great drop of DGs' total output occurs, the reactive power transmitted from the grid is 0 because of the control of the SST input stage, while the active power is −0.2 MW because of the plenty outputs of DGs. After the total output of DGs drops to 0, the low voltage distribution network supplies a certain amount of powers to help to maintain the bus voltage at this moment.

6. Conclusions

The development of the technology of DGs has realized the effective integration and efficient utilization of renewable energies distributed around the world. It has practical significance to study on the transient voltage stability of the DGs grid-connected system and it is meaningful for realizing the change from a traditional fossil-fuel grid to a future green smart grid. In this paper, we use PSCAD software to study the transient voltage stability of the low voltage distributed network integrated with DGs based on SST under the condition of cable line fault and sudden drop of DGs' total output and concluded as follows:

(1) Using a SST for the integration of DGs and the distribution network has advantages on the system transient voltage stability while facing different faults. The influence of grid-side line short circuit fault on the transient voltage stability is related to fault location, and the line disconnection fault is not the case. Even if SST has to regulate the voltage passively when the fault occurs at the line close to the SST input stage, the regulation function of SST still can maintain the voltage transient stability of load bus. This avoids load bus in the conventional DGs gird-connected system losing its transient voltage stability effectively while facing such faults and improves utilization of DGs and reliability of power supply.

(2) Although the SST control makes the load bus have better transient voltage stability, the DC bus voltage is easy to keep climbing continually when the short circuit occurs at the line side that is close to the SST input stage or the line disconnection occurs at any location of the line. At this moment, the DC bus can be considered to be transient voltage instability, and this is a new transient voltage stability phenomenon in the DGs gird-connected system using SST. It is harmful to the security and stability of the system

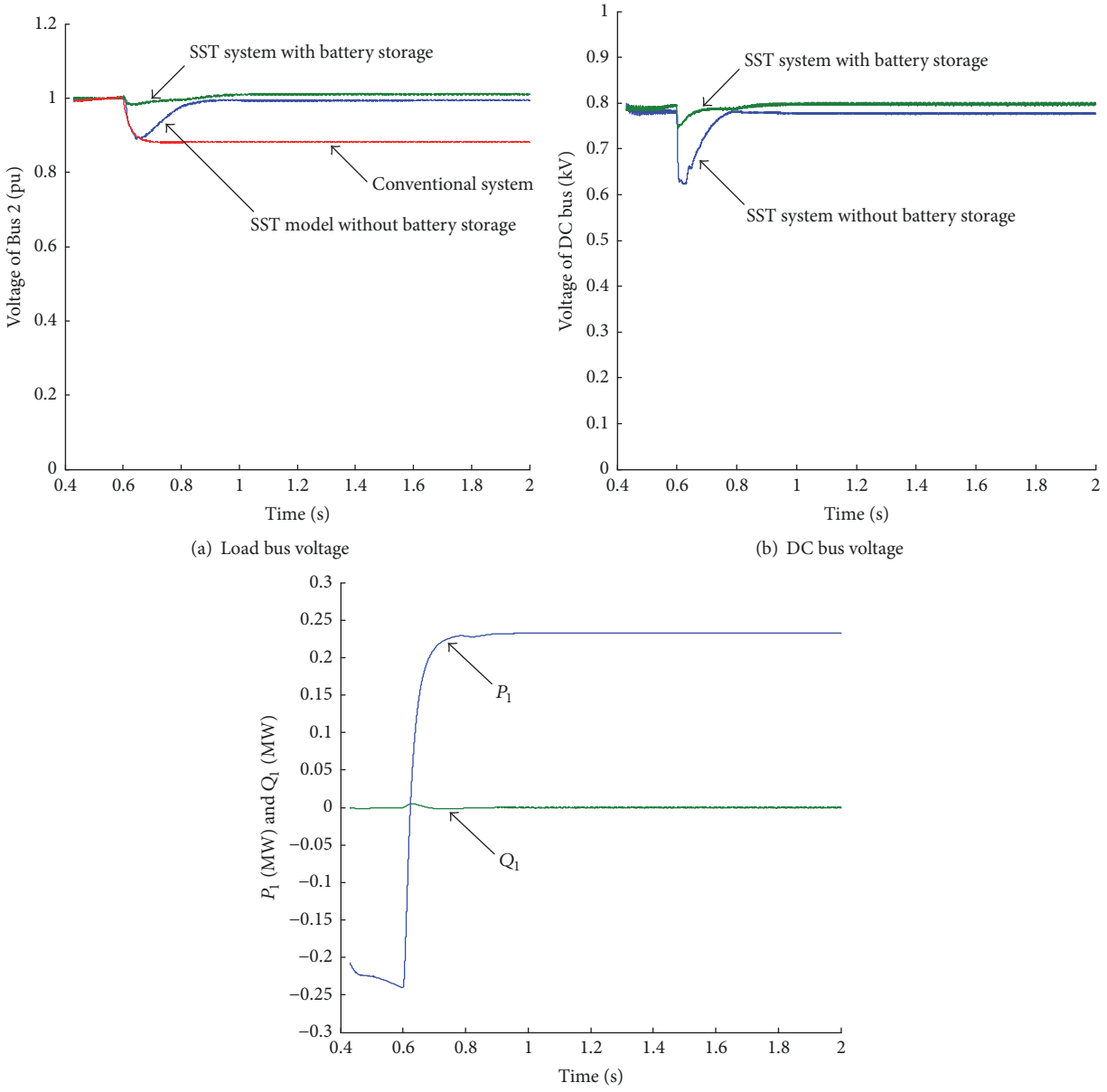

(a) Load bus voltage

(b) DC bus voltage

(c) Power supplies of distribution network without battery storage

Figure 9: Response curves when total output of DGs drops to 0.

operation. The DC bus voltage can be stabilized by the DGs equipped with a certain amount of batteries or a battery energy storage station installed in the DC bus when faults occur, which can effectively avoid the transient voltage instability of DC bus and guarantee the system safety.

(3) When the total output of DGs drops greatly under the adverse weather condition, the SST can ensure the transient voltage stability thus avoiding the biggest voltage drop of load bus in the conventional system. If a battery energy storage station is installed, the load bus voltage and DC bus voltage will be almost unaffected while facing the great drop of the DGs' total output. It is of great significance to the stable operation of low voltage distribution network that the battery storage is installed.

Data Availability

The data used to support the findings of this study are available from the corresponding author upon request.

Conflicts of Interest

The authors declare that there are no conflicts of interest regarding the publication of this paper.

Acknowledgments

This work is supported by the Open Research Fund of Jiangsu Collaborative Innovation Center for Smart Distribution Network (XTCX201613), the University Student Innovation & Entrepreneurship Training Program of Jiangsu Province (201711276009Z), and the University Student Technological Innovation Project of Nanjing Institute of Technology (TZ20170009).

References

[1] S. Li, Z. Wei, Y. Ma, and J. Cheng, "Prediction and control of Hopf bifurcation in a large-scale PV grid-connected system based on an optimised support vector machine," *The Journal of Engineering*, vol. 2017, no. 14, pp. 2666–2671, 2017.

[2] A. Eid and M. Abdel-Akher, "Voltage control of unbalanced three-phase networks using reactive power capability of distributed single-phase PV generators," *International Transactions on Electrical Energy Systems*, vol. 27, no. 11, Article ID e2394, 2017.

[3] A. Q. Huang, M. L. Crow, G. T. Heydt, J. P. Zheng, and S. J. N. I. S. Dale, "The Future Renewable Electric Energy Delivery and Management (FREEDM) System: The Energy Internet," *Proceedings of the IEEE*, 2010.

[4] J. M. Sexauer and S. Mohagheghi, "Voltage quality assessment in a distribution system with distributed generation-a probabilistic load flow approach," *IEEE Transactions on Power Delivery*, vol. 28, no. 3, pp. 1652–1662, 2013.

[5] S. Li, Z. Wei, and Y. Ma, "Fuzzy Load-Shedding Strategy Considering Photovoltaic Output Fluctuation Characteristics and Static Voltage Stability," *Energies*, vol. 11, no. 4, p. 779, 2018.

[6] J. Cao and M. Yang, "Energy internet-towards smart grid 2.0," in *Proceedings of the 2013 Fourth International Conference on Networking and Distributed Computing (ICNDC)*, pp. 105–110, Los Angeles, CA, USA, December 2013.

[7] W. Sheng, H. Liu, Z. Zeng et al., "An energy hub based on virtual-machine control," in *Proceedings of the CSEE*, vol. 35, pp. 3541–3550, 2015.

[8] . Qing Duan, . Chunyan Ma, . Wanxing Sheng, and . Changkai Shi, "Research on power quality control in distribution grid based on energy router," in *Proceedings of the 2014 International Conference on Power System Technology (POWERCON)*, pp. 2115–2121, Chengdu, October 2014.

[9] B. Tamimi, C. Canizares, and K. Bhattacharya, "System stability impact of large-scale and distributed solar photovoltaic generation: The case of Ontario, Canada," *IEEE Transactions on Sustainable Energy*, vol. 4, no. 3, pp. 680–688, 2013.

[10] R. Majumder, "Some aspects of stability in microgrids," *IEEE Transactions on Power Systems*, vol. 28, no. 3, pp. 3243–3252, 2013.

[11] R. Yan and T. K. Saha, "Investigation of voltage stability for residential customers due to high photovoltaic penetrations," *IEEE Transactions on Power Systems*, vol. 27, no. 2, pp. 651–662, 2012.

[12] S. Li, C. Jiang, Z. Zhao, and Z. Li, "Study of transient voltage stability for distributed photovoltaic power plant integration into low voltage distribution network," *Dianli Xitong Baohu yu Kongzhi/Power System Protection and Control*, vol. 45, no. 8, pp. 67–72, 2017.

[13] M. M. Aly, M. Abdel-Akher, Z. Ziadi, and T. Senjyu, "Assessment of reactive power contribution of photovoltaic energy systems on voltage profile and stability of distribution systems," *International Journal of Electrical Power & Energy Systems*, vol. 61, pp. 665–672, 2014.

[14] A. Eid, "Utility integration of PV-wind-fuel cell hybrid distributed generation systems under variable load demands," *International Journal of Electrical Power & Energy Systems*, vol. 62, pp. 689–699, 2014.

[15] Y. K. Gounder, D. Nanjundappan, and V. Boominathan, "Enhancement of transient stability of distribution system with SCIG and DFIG based wind farms using STATCOM," *IET Renewable Power Generation*, vol. 10, no. 8, pp. 1171–1180, 2016.

[16] A. Huang and J. Baliga, "FREEDM system: role of power electronics and power semiconductors in developing an energy internet," in *Proceedings of the 21st International Symposium on Power Semiconductor Devices IC's (ISPSD*, pp. 9–12, Barcelona, Spain, 2009.

[17] Y. Ye, M. Kazerani, and V. Quintana, "A novel modeling and control method for three-phase PWM converters," in *Proceedings of the 2001 IEEE 32nd Annual Power Electronics Specialists Conference*, pp. 102–107, Vancouver, BC, Canada.

[18] F. Wang, A. Huang, G. Wang, X. She, and R. Burgos, "Feedforward control of solid state transformer," in *Proceedings of the 2012 IEEE Applied Power Electronics Conference and Exposition - APEC 2012*, pp. 1153–1158, Orlando, FL, USA, Feburary 2012.